Carrier-Density-Induced Ferromagnetism in EuTiO₃ Bulk and Heterostructures

Zhigang Gui and Anderson Janotti®

Department of Materials Science and Engineering, University of Delaware, Newark, Delaware 19716, USA

(Received 5 September 2018; published 17 September 2019)

EuTiO₃ is an antiferromagnetic (AFM) material showing strong spin-lattice interactions, large magnetoelectric response, and quantum paraelectric behavior at low temperatures. Using electronic-structure calculations, we show that adding electrons to the conduction band leads to ferromagnetism. The transition from antiferromagnetism to ferromagnetism is predicted to occur at \sim 0.08 electrons/Eu (\sim 1.4 × 10²¹ cm⁻³). This effect is also predicted to occur in heterostructures such as LaAlO₃/EuTiO₃, where ferromagnetism is triggered by the formation of a high-density two-dimensional electron gas in the EuTiO₃. Our analysis indicates that the coupling between Ti 3d and Eu 5d plays a crucial role in lowering the Ti 3d conduction band in the ferromagnetic (FM) phase, leading to an almost linear dependence of the energy difference between the FM and AFM ordering on the carrier concentration. These findings open up possibilities in designing field-effect transistors using EuTiO₃-based heterointerfaces to probe fundamental interactions between highly localized spins and itinerant, polarized charge carriers.

DOI: 10.1103/PhysRevLett.123.127201

The coupling between spin, lattice, and charge in complex oxides gives rise to extremely rich phase diagrams including magnetism, ferroelectricity, magnetoelectricity, superconductivity, and colossal magnetoresistance [1,2]. The combination of these 3 degrees of freedom is found in rare-earth titanates where itinerant Ti 3d electrons couple with localized rare-earth 4f electrons, in the presence of TiO₆ octahedral tilt and rotations [3]. Advances in epitaxial growth of oxide-based heterostructures, with meticulous control of thickness down to a monatomic layer, have enabled the study of the cross-coupling of these interactions. Recently, an electric-field-tunable spin-polarized and superconducting quasi-2D electron system was created by inserting a few unit-cell thick layer of EuTiO₃ at the LaAlO₃/SrTiO₃ interface [4]. The LaAlO₃/ EuTiO₃/SrTiO₃ δ -doped heterostructure was found to display different ground states depending on the carrier density, from Kondo-like transport at low carrier concentrations, to superconductivity and itinerant ferromagnetism as the 2D carrier density increases, with an intriguing transition from ferromagnetic to superconducting as a function of temperature. It is unclear whether a 2D superconducting state with unconventional order parameter is established as a result of the spin polarization of the itinerant Ti 3d electrons, or ferromagnetism and superconductivity coexist but at different depths inside the quasi-2D electron system [4]. Unraveling the interactions between the itinerant Ti-3d and the localized Eu-4f electrons is key to understanding these observations.

Electronic structure calculations are employed to investigate how excess electrons in the bulk of $EuTiO_3$ and at the $LaAlO_3/EuTiO_3$ interface affect the ordering of the Eu-4f spins. As shown in Fig. 1, we find that a transition from

G-type antiferromagnetic (AFM) to ferromagnetic (FM) ordering occurs as the carrier concentration increases. The fundamental interactions underlaying the FM ordering are explained in terms of orbital couplings. We also show that the two-dimensional electron gas (2DEG) in EuTiO₃/LaAlO₃ heterostructures also makes the EuTiO₃ ferromagnetic, which we attribute to the favored band alignment and charge transfer across the LaO-TiO₂ interface.

Our calculations are based on the density functional theory (DFT) [5,6] and the HSE06 hybrid functional [7,8] as implemented in the VASP code [9]. We use projected augmented wave potentials [10] with the plane-wave basis set with a cutoff of 550 eV. For integrations over the Brillouin zone, we use a $7 \times 7 \times 5$ k-point mesh for bulk

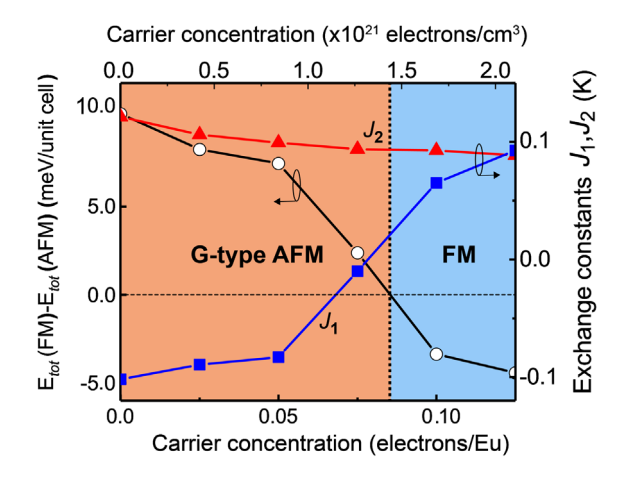


FIG. 1. Total-energy difference between the FM and G-AFM orderings, and first and second nearest-neighbor exchange constants, J_1 and J_2 , as a function of carrier concentration in EuTiO₃.

20-atom cells and $3 \times 3 \times 1$ for the EuTiO₃/LaAlO₃ superlattices (composed of seven unit-cell thick EuTiO₃ and three unit-cell thick LaAlO₃). The atomic positions are fully relaxed until the forces on each atom are less than 0.005 eV/Å and total-energy differences between consecutive steps are less than 10^{-6} eV. In the bulk calculations of the FM and AFM orderings, the lattice parameters and atomic positions are fully relaxed. For the EuTiO₃/LaAlO₃ superlattices, the in-plane lattice parameters were kept fixed during the structural relaxation to mimic the epitaxial growth on a SrTiO₃ substrate. Testing calculations based on DFT + U [11–13] demonstrate robustness of our results and conclusions (Supplemental Material [14]).

EuTiO₃ has a perovskite crystal structure with lattice parameters very close to those of SrTiO₃. In contrast to SrTiO₃, EuTiO₃ is magnetic, with a high spin S = 7/2 per Eu $(4f^7)$. At temperatures lower than 5 K, EuTiO₃ displays G-type AFM ordering [15–17]. Above 5 K, EuTiO₃ becomes paramagnetic. DFT calculations and experiments have demonstrated that epitaxial EuTiO₂ thin films show FM ordering under tensile strain [13,18–21], opening the door to higher-temperature implementations of strong ferromagnetic ferroelectrics and, potentially, to various device applications such as magnetic sensors, high-density multistate memory elements, tunable microwave filters, phase shifters, and resonators. The use of epitaxial strain to stabilize the FM ordering has its limitations, relying on the speed of lattice response for switching between FM and AFM. Here, instead, we turn to doping as a way of controlling the magnetic ordering; i.e., we investigate how charge carriers affect the ordering of the Eu spin moments. Changing the doping level through a gated structure would allow for controlling the magnetization and exploring the fundamental interactions between itinerant electrons and highly localized spin moments.

For studying the effects of charge carriers in EuTiO₃, we added electrons to the perfect bulk represented by a unit cell containing 20 atoms, which allows for the description of both FM and G-type AFM orderings, including the effects of octahedral tilt and rotations. The excess electrons are compensated by a homogeneous neutralizing background to ensure the system is charge neutral. We chose to add electrons to the conduction band, instead of explicitly adding shallow-donor impurities, to separate the effects of excess charge carriers from the chemical or size effects of the impurities. Possible ways of doping, such as incorporation of impurities and through polar-nonpolar interfaces in heterostructures are discussed.

The spin configuration of the *G*-type AFM ordering in EuTiO₃ is shown in Fig. 2. In both AFM and FM EuTiO₃, there is a small antiphase octahedral rotation around the *c* axis. The calculated lattice parameters for the *G*-type AFM ground state are a = 3.888 Å, c = 3.924 Å, and $\alpha = 7.24^{\circ}$, in good agreement with the experimental values a = 3.903 Å, c = 3.908 Å, and $\alpha = 3.03^{\circ}$ [22,23]. The lattice

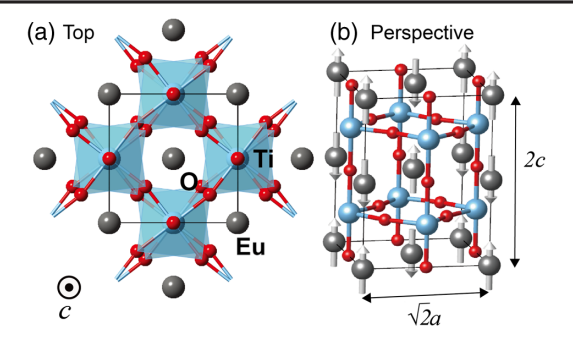


FIG. 2. Ball and stick model of the 20-atom unit cell of $EuTiO_3$ seen (a) from the [001] direction with antiphase rotations of oxygen octahedra around the c axis; (b) perspective view of the G-AFM ordering.

parameters for the FM ordering are a = 3.888 Å, c = 3.926 Å, and $\alpha = 7.23^{\circ}$, i.e., very close to those of the AFM ground state. Doping within the range considered in the present work, i.e., up to 0.125 electrons/Eu, leads to negligible changes in lattice parameters, of less than 0.68%.

To understand the effects of carriers on the magnetic ordering, we first analyze the electronic structure of undoped EuTiO₃. The band structure of the *G*-AFM and FM orderings are shown in Fig. 3. The AFM and FM configurations display a band gap, which is slightly smaller in the FM than in the AFM, and in both cases, we find a magnetic moment of S = 7/2/Eu. The gap separates the occupied narrow Eu-4f band from the unoccupied conduction band derived mostly from Ti-3d orbitals. The O-2p band is about 2 eV below the occupied Eu-4f band. These results are in good agreement with previous HSE06 calculations and photoemission measurements [20], as well

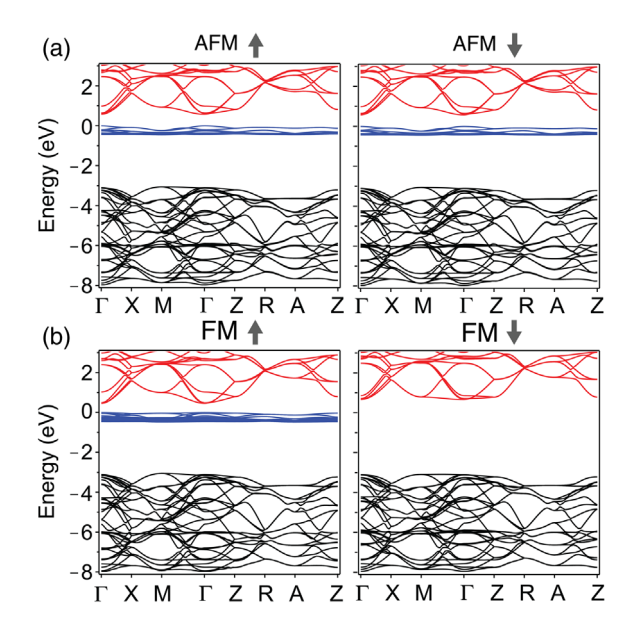


FIG. 3. Electronic band structures of $EuTiO_3$ for (a) G-type AFM ordering, and (b) FM ordering. The zero in the energy axis was set to the top of the occupied Eu-4f band.

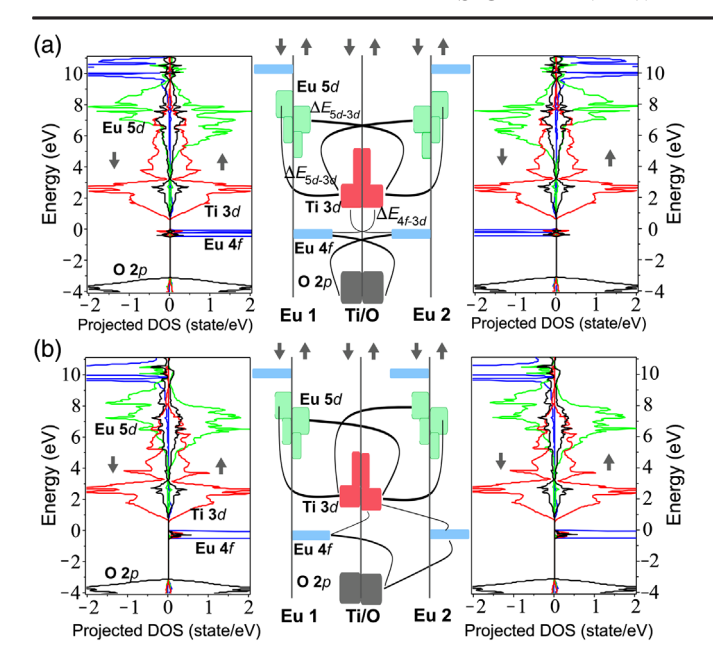


FIG. 4. Density of states projected on Eu-4f orbitals (blue), Eu-5d orbitals (green), Ti-3d orbitals (red), and O-2p orbitals (black), and the derived interband coupling diagrams for the (a) G-type AFM and (b) FM ordering of undoped EuTiO₃. In the interband coupling diagrams, the solid curvy arrows indicate the most relevant couplings. The exchange splitting in the O-2p bands and Ti-3d bands are enlarged for ease of representation. The zero in the energy axis was set to the maximum of the occupied Eu-4f band.

as diffusive reflectance [17] and absorption [24,25] spectra. We also find a significant contribution from Eu 5d to the lowest-energy conduction bands, which suggests a coupling with Ti 3d, as seen in the orbital-projected density of states in Fig. 4. For the undoped case, we find the G-AFM to be lower in energy than the FM ordering by 10.3 meV per unit cell, consistent with previous studies [13,15–21]. It is noteworthy that the conduction-band minimum (CBM) of the FM phase is lower than that of the AFM, i.e., $\Delta E_{\rm CBM} = -0.10$ eV. which we determine following Ref. [26].

By inspecting the band structures in Fig. 3, we note that the excess electrons will be occupying the Ti 3d conduction band. We also note that the exchange splitting at the CBM gives a net polarization to the excess electrons, which is aligned with the FM ordering of the Eu spins. As electrons are added to EuTiO₃, the total-energy difference between the FM and AFM phases $[\Delta E_{\rm FM-AFM} = E_{\rm tot}({\rm FM}) - E_{\rm tot}({\rm AFM})]$ decreases (Fig. 1). When the added electron concentration exceeds 0.08 electrons/Eu $(1.4 \times 10^{21} \, {\rm electrons/cm^3})$, the FM becomes more energetically favorable than the AFM ordering $(\Delta E_{\rm FM-AFM} < 0)$. The monotonic decrease of $\Delta E_{\rm FM-AFM}$ with the excess carriers and the negative sign of $\Delta E_{\rm CBM}$ suggest a simple rigid-band filling model: as electrons are added to the conduction band, the FM ordering will become more stable

than the AFM when $n \times |\Delta E_{\rm CBM}| > \Delta E_{\rm FM-AFM}$, where n is the carrier concentration. From this simple picture, the estimated electron concentration that would make the FM more stable amounts to n=0.03 electrons/Eu, in reasonable agreement with the direct calculated value of n=0.08 electrons/Eu shown in Fig. 1. A comparison of the electronic band structures of the undoped and doped EuTiO₃ (see Supplemental Material [14]) shows that the bands remain intact upon doping, corroborating the rigid-band filling picture.

Why is the CBM in the FM phase lower than that in AFM in EuTiO₃, i.e., $\Delta E_{\rm CBM} < 0$? We explain it based on the coupling between the Ti-3d (t_{2q}) and the Eu-5d (t_{2q}) , Eu-4f, and O-2p bands, of which the Eu 5d-Ti 3d and Eu 4f-Ti 3d are the most relevant because they act differently in the case of the AFM and FM orderings. From the orbital-projected DOS, we constructed the interband interaction diagrams shown in Fig. 4, where we highlight the relevant couplings that affect the position of the Ti-3d band. The energy shift of the Ti-3d band due these couplings is denoted as $\Delta E_{5d-3d}^{X}(\uparrow;1,2)$, $\Delta E_{5d-3d}^{X}(\downarrow;1,2), \ \Delta E_{4f-3d}^{X}(\uparrow;1,2), \ \Delta E_{4f-3d}^{X}(\downarrow;1,2), \ \text{where}$ \uparrow or \downarrow indicate the spin channel, X refers to the AFM or FM ordering, and 1 or 2 represents the index of the two nearest Eu atoms to a given Ti atom. Thus, the spin-up Ti-3d band of the AFM ordering is shifted according to

$$\Delta^{\mathrm{AFM}} = \Delta E_{4f-3d}^{\mathrm{AFM}}(\uparrow;1) - \Delta E_{5d-3d}^{\mathrm{AFM}}(\uparrow;1) - \Delta E_{5d-3d}^{\mathrm{AFM}}(\uparrow;2), \tag{1}$$

where we neglected $\Delta E_{4f-3d}^{\mathrm{AFM}}(\uparrow;2)$ due to the large energy separation between the Ti-3d band and the empty Eu-4f band, and the small overlap of the Ti-3d and Eu-4f orbitals due to the large distance between the Ti and Eu atoms. An equivalent expression can be written for the spin-down Ti-3d band.

For the FM ordering, the spin-up Ti-3d band is shifted according to

$$\Delta^{\mathrm{FM}} = \Delta E_{4f-3d}^{\mathrm{FM}}(\uparrow; 1) + \Delta E_{4f-3d}^{\mathrm{FM}}(\uparrow; 2) - \Delta E_{5d-3d}^{\mathrm{FM}}(\uparrow; 1) - \Delta E_{5d-3d}^{\mathrm{FM}}(\uparrow; 2).$$
 (2)

We note that $E_{5d-3d}^{\text{FM}}(\uparrow;1) = E_{5d-3d}^{\text{FM}}(\uparrow;2) \approx \Delta E_{5d-3d}^{\text{AFM}}(\uparrow;1) \gg \Delta E_{5d-3d}^{\text{AFM}}(\uparrow;2)$. Based on the DOS shown in Fig. 4, and Eqs. (1) and (2), we conclude that the Eu 5*d*-Ti 3*d* coupling is responsible for lowering the Ti-3*d* band in the FM compared to that in the AFM ordering.

In the case of undoped $EuTiO_3$, it has been proposed that the competition between the antiferromagnetic superexchange and an indirect ferromagnetic exchange via the Eu-5d states leads to a delicate balance between the AFM and FM phases [20]. Here, we show how this competition between the AFM and FM orderings is altered by the

presence of electrons in the Ti-3d conduction band. Basically, adding electrons to the conduction band favors the FM phase because its CBM is lower than that in the AFM phase.

It could also be argued that the stabilization of the FM ordering upon doping in EuTiO₃ follows the Stoner model [27]. As the doping concentration in the Ti-3d t_{2g} bands increases, the density of states at the Fermi level increases; at a certain doping concentration, the spin splitting of the Ti-3d bands becomes energetically favorable (since it reduces the electron-electron repulsion), which is consistent with the Stoner picture of magnetism [27]. However, it is important to note that the spin splitting of the Ti-3d bands is already present in the FM undoped EuTiO₃. The polarized Eu-4f bands lead to the spin polarization of the Eu-5d bands, which are composed of orbitals that are quite delocalized in space and overlap with Ti-3d orbitals, thus, leading to a spin-split conduction band. In the rigid-band filling model, adding electrons then lowers the energy of the FM with respect the AFM ordering.

How can electrons be added to the conduction band of EuTiO₃ and how to control their concentration? A conventional method of adding electrons to the conduction band of a semiconductor is to incorporate shallow-donor impurities. These are atoms that typically sit to the right of the host atoms in the periodic table. For EuTiO₃, there are a few possibilities: trivalent impurities sitting on the Eu site, such as Gd and La, pentavalent impurities sitting on the Ti site, such as Nb, or F sitting on the O site. In addition, one could incorporate H, either as interstitial bonded to O, or substitutional replacing O atoms. Both forms have been reported to act as shallow donors in many oxides [28,29].

Experimentally, it has been found that EuTiO₃ doped with either La, Gd, Dy, Nb, or H leads to ferromagnetism [30–34]. It has also been reported that controlling oxygen partial pressure leads to conducting ferromagnetic films [35]. Specifically, EuTiO_{3-x}H_x, with x as low as 0.07, leads to ferromagnetic powders and thin films [34], and that ferromagnetism is observed in EuTi_{1-x}Nb_xO₃ for $x \ge 0.1$ [33]. These results are in good agreement with our predicted AFM-FM transition at ~0.08 electrons/Eu. In all these reports, the emergence of ferromagnetism in doped EuTiO₃ has been attributed to the Ruderman-Kittel-Kasuya-Yosida (RKKY) interaction, yet without any further justification. RKKY is often used to explain the exchange interaction between itinerant electrons and localized magnetic moments. Here, we find that the interaction between the Ti 3d and Eu 4f is of secondary importance, and that the Eu 5*d*-Ti 3*d* coupling (Fig. 4) is key to stabilizing the FM ordering with increasing carrier concentration.

We can also add conduction electrons to $EuTiO_3$ through a heterointerface. In analogy to $LaAlO_3/SrTiO_3(001)$ [36–40], or $GdTiO_3/SrTiO_3(001)$ [41], we predict that a 2DEG will form at the $LaAlO_3/EuTiO_3$ with $LaO-TiO_2$ termination. In such systems, the charge transfer to the

EuTiO₃ layer occurs due to the valence mismatch and the band alignment at the interface [38–40]. The conduction band in the band insulator LaAlO₃ or in the Mott insulator GdTiO₃ lie higher in energy than the conduction band in EuTiO₃ such that, at the LaO-TiO₂ termination, the excess electrons from the LaO donor layer is accommodated in the conduction band of EuTiO₃ [26].

Basically, LaAlO₃ can be thought of as composed of alternating charged planes (LaO)⁺ and (AlO₂)⁻ along the [001] direction, whereas EuTiO₃ is composed of chargeneutral planes (EuO)⁰ and (TiO₂)⁰. In the LaAlO₃, each (LaO)⁺ gives $0.5e^-$ per unit-cell area to the right and $0.5e^-$ to the left (AlO₂)⁻, as indicated in Fig. 5(a). Thus, at the LaO-TiO₂ interface, there will be an excess of $0.5e^-$ per unit-cell area, which, due to the conduction-band offset, is accommodated on the EuTiO₃ side, forming a 2DEG near the interface. The excess electrons from the 2DEG are sufficient to turn the EuTiO₃ layer ferromagnetic.

To demonstrate this effect, we first calculated the band alignment between $LaAlO_3$ and $EuTiO_3$, following the procedure described in [26]; the result is shown in Fig. 5(b). Then, we performed calculations for a $LaAlO_3/EuTiO_3(001)$ superlattice with two equivalent $LaO-TiO_2$ interfaces. The structure of the superlattice $LaAlO_3/EuTiO_3$ is given in Fig. 5(c). The distribution

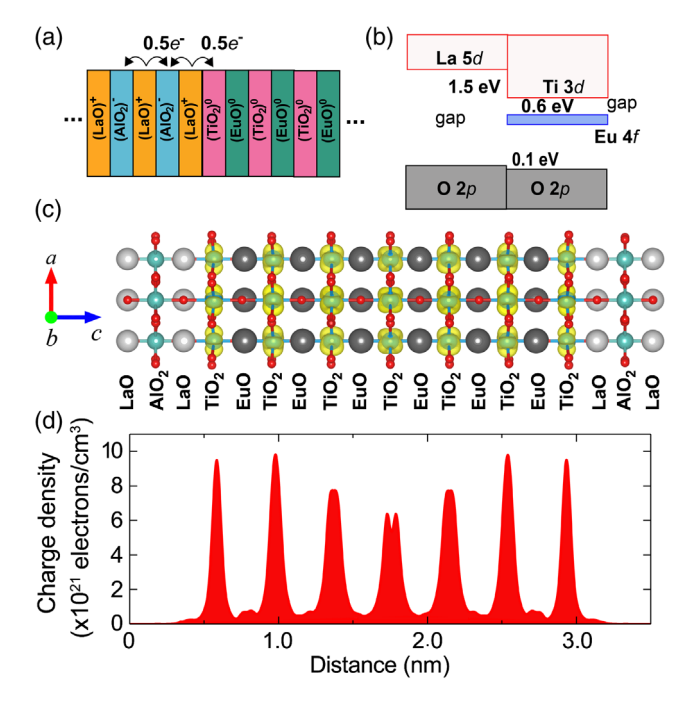


FIG. 5. (a) Formation of a 2DEG at the LaAlO₃/EuTiO₃(001) interface with a LaO-TiO₂ termination. (b) Band alignment at the LaAlO₃/EuTiO₃. (c) Distribution of the charge carriers in the LaAlO₃/EuTiO₃(001) superlattice with two equivalent LaO-TiO₂ interfaces, with the isosurface set to 20% of the maximum value. (d) Planar-averaged excess charge as a function of the distance along the c axis of the superlattice in (c), showing excess charge accumulation in the EuTiO₃.

of the excess charges in the $EuTiO_3$ layer is also shown in Fig. 5(c) and the planar-averaged excess charge density along the c axis is shown in Fig. 5(d).

We find that the FM is lower than the AFM ordering by 9.7 meV/(unit cell) in the heterostructure, and that each Eu atom in the heterostructure holds a magnetic spin moment of S = 7/2/Eu (4 f^7). Considering the thickness of the EuTiO₃ layer (23.5 Å), we obtain an excess electron concentration of $2.4 \times 10^{21} e^{-/\text{cm}^3}$ since each interface gives 0.5 electron per unit cell area. Thus, the stability of the FM ordering is explained by the presence of the excess electrons in the conduction band of EuTiO₃, consistent with the results for bulk shown in Fig. 1. The excess electrons are uniformly distributed over the Ti-3d orbitals in EuTiO₃, contributing with negligibly small moments to the total spin. Our results also explain the observed ferromagnetism in the LaAlO₃/EuTiO₃/SrTiO₃ δ-doped heterostructures [4], which arises from the charge transfer through the LaAlO₃/EuTiO₃ interface.

The results for the LaAlO₃/EuTiO₃(001) in Fig. 5 suggest that the ferromagnetism in the EuTiO₃-based heterostructures could be controlled by an electric field. In a field-effect transistor design, and at low temperatures, an electric field applied through a gate electrode could be used to deplete or accumulate charge carriers in the EuTiO₃ layer near the interface, inducing FM-AFM transitions, thus, enabling the control of the magnetic ordering through a gate voltage. Such a FET has already been demonstrated in the case of LaAlO₃/SrTiO₃ [37,42] and GdTiO₃/SrTiO₃ [43], although a complete depletion of the excess charge in the SrTiO₃ layer has proved challenging. Such a device could be used to manipulate and control the magnetic ordering in EuTiO₃ thin films and, also, to investigate the fundamental interactions between the electrons in the 2DEG with the large Eu spin moments near the interface through the current between source and drain.

This work was funded by the NSF Early Career Award Grant No. DMR-1652994. We used the computing resources provided by the Extreme Science and Engineering Discovery Environment (XSEDE), supported by National Science Foundation Grant No. ACI-1053575, and the high-performance computing resources at the University of Delaware.

- [1] H. Y. Hwang, Y. Iwasa, M. Kawasaki, B. Keimer, N. Nagaosa, and Y. Tokura, Nat. Mater. 11, 103 (2012).
- [2] W. Eerenstein, N. D. Mathur, and J. F. Scott, Nature (London) **442**, 759 (2006).
- [3] J. B. Goodenough and J.-S. Zhou, in *Localized to Itinerant Electronic Transition in Perovskite Oxides* (Springer, Berlin, 2001), Vol. 98, pp. 17–113.
- [4] D. Stornaiuolo, C. Cantoni, G. M. De Luca, R. Di Capua, E. Di Gennaro, G. Ghiringhelli, B. Jouault, D. Marrè, D. Massarotti, F. Miletto Granozio, I. Pallecchi, C. Piamonteze,

- S. Rusponi, F. Tafuri, and M. Salluzzo, Nat. Mater. **15**, 278 (2016).
- [5] P. Hohenberg and W. Kohn, Phys. Rev. 136, B864 (1964).
- [6] W. Kohn and L. J. Sham, Phys. Rev. 140, A1133 (1965).
- [7] J. Heyd, G. E. Scuseria, and M. Ernzerhof, J. Chem. Phys. 118, 8207 (2003).
- [8] A. V. Krukau, O. A. Vydrov, A. F. Izmaylov, and G. E. Scuseria, J. Chem. Phys. 125, 224106 (2006).
- [9] G. Kresse and J. Furthmüller, Phys. Rev. B 54, 11169 (1996).
- [10] P. E. Blöchl, Phys. Rev. B 50, 17953 (1994).
- [11] J. P. Perdew, A. Ruzsinszky, G. I. Csonka, O. A. Vydrov, G. E. Scuseria, L. A. Constantin, X. Zhou, and K. Burke, Phys. Rev. Lett. 100, 136406 (2008).
- [12] V. I. Anisimov, F. Aryasetiawan, and A. I. Lichtenstein, J. Phys. Condens. Matter 9, 767 (1997).
- [13] Y. Yang, W. Ren, D. Wang, and L. Bellaiche, Phys. Rev. Lett. 109, 267602 (2012).
- [14] See Supplemental Material at http://link.aps.org/supplemental/10.1103/PhysRevLett.123.127201 for details on the DFT + *U* calculations, band structures and projected DOS of EuTiO₃ for the *G*-type AFM and FM orderings (with and without doping), the variation of the lattice parameters with doping concentration, and the determination of the exchange constants *J*₁ and *J*₂.
- [15] T. R. McGuire, M. W. Shafer, R. J. Joenk, H. A. Alperin, and S. J. Pickart, J. Appl. Phys. 37, 981 (1966).
- [16] C.-L. Chien, S. DeBenedetti, and F. D. S. Barros, Phys. Rev. B 10, 3913 (1974).
- [17] H. Akamatsu, K. Fujita, H. Hayashi, T. Kawamoto, Y. Kumagai, Y. Zong, K. Iwata, F. Oba, I. Tanaka, and K. Tanaka, Inorg. Chem. **51**, 4560 (2012).
- [18] C. J. Fennie and K. M. Rabe, Phys. Rev. Lett. **97**, 267602 (2006).
- [19] J. H. Lee et al., Nature (London) 466, 954 (2010).
- [20] H. Akamatsu, Y. Kumagai, F. Oba, K. Fujita, H. Murakami, K. Tanaka, and I. Tanaka, Phys. Rev. B 83, 214421 (2011).
- [21] K. Tanaka, K. Fujita, Y. Maruyama, Y. Kususe, H. Murakami, H. Akamatsu, Y. Zong, and S. Murai, J. Mater. Res. 28, 1031 (2013).
- [22] T. Katsufuji and H. Takagi, Phys. Rev. B 64, 054415 (2001).
- [23] J. Köhler, R. Dinnebier, and A. Bussmann-Holder, Phase Trans. **85**, 949 (2012).
- [24] J. H. Lee, X. Ke, N. J. Podraza, L. F. Kourkoutis, T. Heeg, M. Roeckerath, J. W. Freeland, C. J. Fennie, J. Schubert, D. A. Muller, P. Schiffer, and D. G. Schlom, Appl. Phys. Lett. 94, 212509 (2009).
- [25] T. Kolodiazhnyi, M. Valant, J. R. Williams, M. Bugnet, G. A. Botton, N. Ohashi, and Y. Sakka, J. Appl. Phys. 112, 083719 (2012).
- [26] L. Bjaalie, B. Himmetoglu, L. Weston, A. Janotti, and C. G. Van de Walle, New J. Phys. 16, 025005 (2014).
- [27] E. C. Stoner, Proc. R. Soc. Ser. A 169, 339 (1939).
- [28] C. G. Van de Walle, Phys. Rev. Lett. 85, 1012 (2000).
- [29] A. Janotti and C. G. Van de Walle, Nat. Mater. 6, 44 (2007).
- [30] T. Katsufuji and Y. Tokura, Phys. Rev. B 60, R15021 (1999).
- [31] K. Yoshii, M. Mizumaki, A. Nakamura, and H. Abe, J. Solid State Chem. **171**, 345 (2003).

- [32] Y. Kususe, H. Murakami, K. Fujita, I. Kakeya, M. Suzuki, S. Murai, and K. Tanaka, Jpn. J. Appl. Phys. 53, 05FJ07 (2014).
- [33] L. Li, J. R. Morris, M. R. Koehler, Z. Dun, H. Zhou, J. Yan, D. Mandrus, and V. Keppens, Phys. Rev. B 92, 024109 (2015).
- [34] T. Yamamoto, R. Yoshii, G. Bouilly, Y. Kobayashi, K. Fujita, Y. Kususe, Y. Matsushita, K. Tanaka, and H. Kageyama, Inorg. Chem. **54**, 1501 (2015).
- [35] K. Kugimiya, K. Fujita, K. Tanaka, and K. Hirao, J. Magn. Magn. Mater. 310, 2268 (2007).
- [36] A. Ohtomo and H. Y. Hwang, Nature (London) 427, 423 (2004).
- [37] S. Thiel, G. Hammerl, A. Schmehl, C. W. Schneider, and J. Mannhart, Science 313, 1942 (2006).

- [38] J. Lee and A. A. Demkov, Phys. Rev. B **78**, 193104 (2008).
- [39] R. Pentcheva and W. E. Pickett, Phys. Rev. B **74**, 035112 (2006).
- [40] A. Janotti, L. Bjaalie, L. Gordon, and C. G. Van de Walle, Phys. Rev. B 86, 241108(R) (2012).
- [41] P. Moetakef, T. A. Cain, D. G. Ouellette, J. Y. Zhang, D. O. Klenov, A. Janotti, C. G. Van de Walle, S. Rajan, S. James Allen, and S. Stemmer, Appl. Phys. Lett. 99, 232116 (2011).
- [42] B. Förg, C. Richter, and J. Mannhart, Appl. Phys. Lett. 100, 053506 (2012).
- [43] M. Boucherit, O. Shoron, C. A. Jackson, T. A. Cain, M. L. C. Buffon, C. Polchinski, S. Stemmer, and S. Rajan, Appl. Phys. Lett. 104, 182904 (2014).